J Therm Anal Calorim (2010) 99:893–898
DOI 10.1007/s10973-009-0487-4

Thermal study of some new Ni(II) and Cu(II) complexes with ligands derived from N,N-dimethylbiguanide as potential antimicrobials

Rodica Olar · Mihaela Badea · Dana Marinescu

MEDICTA2009 Conference

Abstract The reaction between $[M(DMBG)_2]\cdot nH_2O$ ((**1**) M:Ni, $n = 0$; (**4**) M:Cu, $n = 1$), ammonia/hydrazine and formaldehyde in methanol resulted in new complexes of type $[ML]\cdot nH_2O$ ((**2**) M:Ni, L:L^1, $n = 0$; (**3**) M:Ni, L:L^2, $n = 0$, (**5**) M:Cu, L:L_1, $n = 0$ and (**6**) M:Cu, L:L_2, $n = 3$; HDMBG: N,N-dimethylbiguanide, L^1 = ligand resulted from ammonia system and L^2 = ligand resulted from hydrazine system). The features of complexes have been assigned from microanalytical, IR and UV–Vis data. The thermal transformations of compounds are complex processes according to TG and DTG curves including melting, phase transition, dehydration, oxidative condensation of –C=N– units as well as thermolysis processes. The final products of decomposition are the most stable metal oxides.

Keywords Complex · N · N-dimethylbiguanide · One pot condensation · Thermal behaviour

Introduction

N,N-dimethylbiguanide (HDMBG) and its complexes present a broad spectrum of biological activity. They act as hypoglycemic agents but display also the analgesic, antimalarial, antimetabolite, cytostatic as well as antimicrobial activity [1–7].

As a species containing the Y-shaped CN_3 unit, in neutral or anionic form, is capable of exhibiting a variety of coordination modes and a range of donor properties leading to compatibility with a remarkably wide range of metal ions, specially that have ability to form square planar complexes as Ni(II) and Cu(II) [8, 9]. A common feature of these systems is that the anionic forms of the ligands that occur in the corresponding neutral divalent metal complexes exhibit self-complementary doublet donor–acceptor (DA) hydrogen bonding motifs [10]. This ability confers to such complexes the ability to interact with biomolecules also. It is worth to mention that the Y-shaped CN_3 unit is component of some bioligands as creatine, creatinine and guanine. This indicates that the biguanide complexes have the ability to selective recognize the biomolecules that contain such units.

It was shown also that the N,N-dimethylbiguanide as well as its complexes, with the neutral or anionic form of the ligand, display an interesting thermal behaviour [4–7]. Moreover, in last years, many studies concerning the Ni(II) and Cu(II) complexes that show a good antimicrobial activity were published [11–19].

In order to improve the biological activity of Ni(II) and Cu(II) complexes with biguanide moiety, new complexes with such units incorporated in a macrocycle have been synthesized and characterized. The thermal behaviour of these derivatives was investigated by thermal analysis (TG, DTA) in order to evidence the modifications appeared at heating and also the thermodynamics effects that accompany them.

Experimental

Materials and methods

All reagents were of commercial analytical quality and have been used without further purification. Chemical

---

R. Olar (✉) · M. Badea · D. Marinescu
Faculty of Chemistry, Department of Inorganic Chemistry,
University of Bucharest, 90-92 Panduri Str., Sector 5,
050663 Bucharest, Romania
e-mail: rodica_m_olar@yahoo.com

analysis of carbon, nitrogen and hydrogen has been performed using a Perkin Elmer PE 2400. Copper was determined using the thiosulphate method while the nickel was determined gravimetrically as dimethylglyoximate.

IR spectra were recorded in KBr pellets with a Bruker Tensor 37 spectrometer in the range 400–4000 cm^{-1}.

Electronic spectra by diffuse reflectance technique, with MgO standard, were recorded in the range 300–1500 nm, on a Jasco V670 spectrophotometer.

The heating curves (TG and DTA) were recorded using a Labsys 1200 SETARAM thermobalance with a sample mass between 5 and 20 mg over the temperature range of 20–900 °C and a heating rate of 10 °C/min. The measurements were carried out in synthetic air atmosphere (flow rate 16.66 cm^3/min) by using alumina crucible.

The melting was evidenced with Automated Melting Point System (AMPS) MPA 100 OptiMelt Stanford Research System.

The X-ray powder diffraction patterns were collected on a DRON-3 diffractometer with a nickel filtered Cu K_α radiation ($\lambda = 1.5418$ Å) in a 2θ range of 5–70°, a step width of 0.05° and an acquisition time of 2 s on each step.

Synthesis and spectral data of the complexes

The syntheses and structural data for complexes $[M(DMBG)_2]$ were reported elsewhere [8, 9]. The composition of complexes has been confirmed by chemical analyses.

Syntheses of the compounds [ML]: To a suspension of [M(DMBG)] (5 mmol) in 100 mL methanol was added drop wise 2 mL formaldehyde (37%) and 5 mL ammonia/hydrazine. The reaction mixture was refluxed 24 h until a sparingly soluble compound was formed. The microcrystalline product was filtered off, washed with EtOH and air-dried.

$[Ni(L^1)]$ (**2**): Analysis, found: Ni, 14.65; C, 36.27; H, 6.51; N, 42.41, $NiC_{12}H_{26}N_{12}$ requires: Ni, 14.78; C, 36.29; H, 6.60; N, 42.33; IR (KBr pellet), cm^{-1}: $\nu_{as}(NH_2)$, 3338m, 3364m; $\nu_s(NH_2)$, 3209m; $\nu_{as}(CH_3)$, 2968w; $\nu_s(CH_3)$, 2890w; ν(C=N), 1685vs, 1650s; $\delta(NH_2)$, 1613m, 1514m; ν(chelate ring), 1341w; ν(C–N), 1123w, 1079w; $\gamma(NH_2)$, 897w, 814w; ν(Ni–N), 425w.

$[Ni(L^2)]$ (**3**): Analysis, found: Ni, 13.68; C, 33.68; H, 6.54; N, 46.03, $NiC_{12}H_{28}N_{14}$ requires: Ni, 13.74; C, 33.74; H, 6.61; N, 45.91, IR (KBr pellet), cm^{-1}: $\nu_{as}(NH_2)$, 3388s, 3364s; $\nu_s(NH_2)$, 3209s; ν(C=N), 1684vs, 1651vs; ν(chelate ring), 1346w; ν(C–N), 1080w; ν(Ni–N), 419w.

$[Cu(L^1)]$ (**5**): Analysis, found: Cu, 15.74; C, 35.77; H, 6.41; N, 41.87, $CuC_{12}H_{26}N_{12}$ requires: Cu, 15.81; C, 35.86; H, 6.52; N, 41.82; IR (KBr pellet), cm^{-1}: $\nu_{as}(NH_2)$, 3400m, 3359m; $\nu_s(NH_2)$, 3209s; ν(C=N), 1678vs, 1646s; ν(chelate ring), 1323w; ν(C–N), 1122w, 1078w ν(Cu–N), 437w.

$[Cu(L^2)]\cdot 3H_2O$ (**6**): Analysis, found: Cu, 12.93; C, 29.58; H, 6.98; N, 40.37, $CuC_{12}H_{34}N_{14}O_3$ requires: Cu, 13.07; C, 29.65; H, 7.05; N, 40.34, IR (KBr pellet), cm^{-1}: ν(OH), $\nu_{as}(NH_2)$, $\nu_s(NH_2)$, 3420vs, large; ν(C=N), 1698vs, 1635s; ν(chelate ring), 1350w; ν(C–N), 1086w; ν(Cu–N), 419w.

Results and discussions

Synthesis and physico-chemical characterization of compounds

In this paper, we report the physico-chemical as well as thermal characterization of N,N-dimethylbiguanidinium (HDMBG) complexes $[M(DMBG)_2]\cdot nH_2O$ ((**1**) M:Ni, $n = 0$; (**4**) M:Cu, $n = 1$), complexes synthesised according to literature data [8, 9]. Manipulation of $[M(DMBG)_2]\cdot nH_2O$ complexes by one pot condensation with ammonia or hydrazine and formaldehyde, has resulted in neutral new complexes $[ML]\cdot nH_2O$ ((**2**) M:Ni, L:L_1, $n = 0$; (**3**) M:Ni, L:L_2, $n = 0$, (**5**) M:Cu, L:L_1, $n = 0$ and (**6**) M:Cu, L:L_2, $n = 3$; L_1 = ligand resulted from ammonia system and L_2 = ligand resulted from hydrazine system).

The IR spectra of complexes reveal the characteristic bands of biguanide moiety. In the range 1630–1700 cm^{-1}, two intense bands characteristic to ν(C=N) vibration mode appears shifted also to higher wavenumbers in the complexes spectra as result of coordination. The new band at about 1350 cm^{-1} can be associated with the chelate ring formation by the biguanide derivatives [20]. The water presence in complexes (**4**) and (**6**) generates a band or a shoulder around 3400 cm^{-1} [21].

Electronic spectra of the complexes show a single narrow band at about 21000 cm^{-1}, as is usually observed for Ni(II) and Cu(II) complexes with a square planar stereochemistry [22].

The coordination proposed for new complexes according with these data together with that known one for complexes (**1**) and (**4**) [8, 9] are presented in Fig. 1.

Thermal behaviour of compounds

The results concerning the thermal degradation in synthetic air of the compounds evidenced difference concerned their thermal behaviour and the general aspect of the TG and DTA curves.

The complex (**1**) is anhydrous so no detectable change in TG curve up to 257 °C is observed. It is worth to mention that in the 119–217 °C range an endothermic effect can be noticed on the DTA curve (Fig. 2; Table 1). This behaviour could be generated by a phase transition as a result of hydrogen bonds reorganization by temperature increasing.

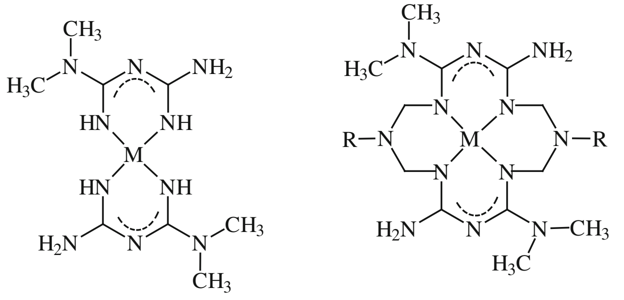

(1) $[Ni(HDMBG)_2]$
(4) $[Cu(HDMBG)_2]\cdot H_2O$

(2) $[Ni(L^1)]$ (R=H)
(3) $[Ni(L^2)]$ ($R=NH_2$)
(5) $[Cu(L^1)]$ (R=H)
(6) $[Cu(L^2)]\cdot 3H_2O$ ($R=NH_2$)

Fig. 1 The known coordination for complexes (**1**) and (**4**) and the proposed one for new complexes

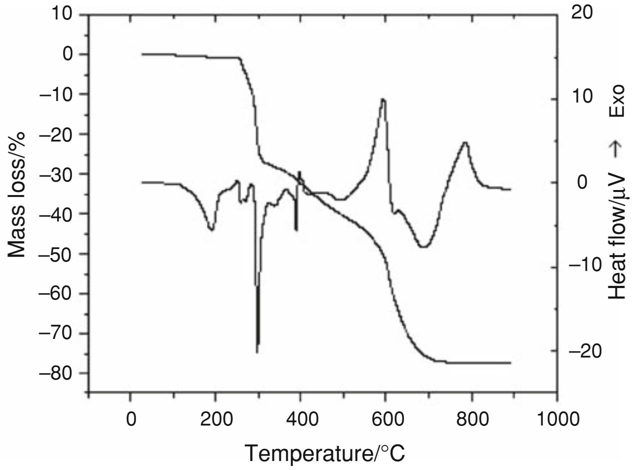

Fig. 2 TG and DTA curves of $[Ni(DMBG)_2]$ (**1**)

Also, after the thermal decomposition starts, the intermediate melts at 286 °C, process evidenced with the Automated Melting Point System (AMPS) also.

According to the mass lost, the intermediate formed after this step is a parcyanide species of type $NiO(CN)_6$. The IR spectrum of this intermediate display indeed the characteristic bands of the paracyanide species at 1617 and 1507 (ν(C=N)), 1340 (ν(C=C)) and 792 cm^{-1}(ν(C–C)) [5–7]. The shoulder at 480 cm^{-1} can be assigned to the ν(Ni–O) vibration mode [22] having in view that in the NiO spectrum this appear as a intense and sharp band at 460 cm^{-1}.

Next step is a very complex one being an overlapping of at least five processes as DTA indicates. This could comprise stepwise depolymerization and oxidative degradation of paracyanide leading finally to the non-stoichiometric nickel(II) oxide (found/calcd. overall mass loss: 76.1/76.3%). The nature of final product was assigned based on IR and powder X-ray diffraction data (ASTM 78-0423). The endothermic effect noticed over 735 °C is associated with the NiO crystallisation.

According to the TG profile the decomposition of complex (**2**) occurs in two steps with nickel oxide as final product (found/calcd. overall mass loss: 80.9/81.2). This species is very stable and the thermal transformation starts with this melting at 272 °C (Fig. 3).

The oxidative degradation starts immediately and the observed mass variation during the first step corresponds to the loss of a part of ligand with $NiO(CN)_8$ formation according to the chemical analysis and IR spectrum. The paracyanide formation generates bands at 1616 (ν(C=N)), 1313 (ν(C=C)) and 787 cm^{-1}(ν(C–C)) in the IR spectrum. The weak band at 526 cm^{-1} can be assigned also to the ν(Ni–O) vibration mode, indicating the generation of this species in the paracyanide network. The final step is an overlapping of at least three processes according to DTA curve.

The anhydrous complex (**3**) is stable up to 187 °C; the endothermic effect observed on the DTA curve in the 86–143 °C range (Fig. 4) is generated by a phase transition. After the thermal decomposition starts, the intermediate melts also at 282 °C. The oxidative degradation occurs in at least two processes (according to both TG and DTA curves) with $NiO(CN)_8$ formation (bands in the IR spectrum at 1617 and 1507 (ν(C=N)), 1340(ν(C=C)), 792(ν(C–C)) and 470 cm^{-1} ν(Ni–O)). The next step is an overlap of five exothermic processes as DTA indicates generating nickel oxide as final product (found/calcd. overall mass loss: 81.9/82.6%).

The same observation can be made for the copper complexes thermal behaviour. The complex (**4**) decomposes in three steps as result of water elimination in the range 88–167 °C (Fig. 5). The low temperatures that correspond to this transformation are an indicative of uncoordinated nature of these water molecules as was observed for other complexes also [23–26].

In the IR spectrum of anhydrous complex isolated at 170 °C, the shoulder at 3310 cm^{-1} assigned to ν(OH) disappears. The decomposition of the anhydrous species starts immediately and comprises three processes, one endo and two exothermic (according to both TG and DTA profiles), the endo one being assigned to an intermediate melting at 219 °C. The ligand degradation occurs also in this step with paracyanide generation as the IR spectrum indicates ((bands at 1533 (ν(C=N)), 1318(ν(C=C)), 783(ν(C–C)) and 472 cm^{-1}, ν(Cu–O). The formed intermediate $CuO(CN)_4$, in the next step leads to CuO as IR (517 cm^{-1}, ν(Cu–O)) and X-ray diffraction indicate (ASTM 5-661) (found/calcd. overall mass loss: 70.4/71.1%). According to both TG and DTA curves, this last step is an overlap of at least three processes.

Table 1 Thermal behaviour of the complexes in synthetic air flow

Compound	Step	Thermal effect	Temperature range/°C	Δm_{exp}/%	Δm_{calc}/%
[Ni(DMBG)$_2$] (**1**)	1.	Endothermic	119–217	0	0
	2.	Miscellaneous	257–328	26.9	26.7
	3.	Exothermic	328–735	49.2	49.6
	Residue NiO			23.9	23.7
[Ni(L^1)] (**2**)	1.	Endothermic	272[a]	0	0
	2.	Exothermic	272–380	28.7	28.8
	3	Exothermic	380–670	52.2	52.4
	Residue NiO			19.1	18.8
[Ni(L^2)] (**3**)	1.	Endothermic	86–143	0	0
	2.	Miscellaneous	187–357	45.3	46.0
	3.	Exothermic	357–600	36.6	36.6
	Residue NiO			18.1	17.5
[Cu(DMBG)$_2$]·H$_2$O (**4**)	1.	Endothermic	88–167	5.3	5.3
	2.	Miscellaneous	167–385	39.7	40.3
	3.	Exothermic	385–605	30.7	30.8
	Residue CuO			29.6	28.9
[Cu(L^1)] (**5**)	1.	Endothermic	210[a]	0	0
	2.	Exothermic	210–326	32.0	32.4
	3.	Exothermic	326–650	47.8	47.8
	Residue CuO			20.2	19.8
[Cu(L^2)]·3H$_2$O (**6**)	1.	Endothermic	60–120	11.0	11.1
	2.	Exothermic	120–330	61.6	61.8
	3.	Exothermic	330–650	10.4	10.7
	Residue CuO			17.0	16.4

[a] Melting point

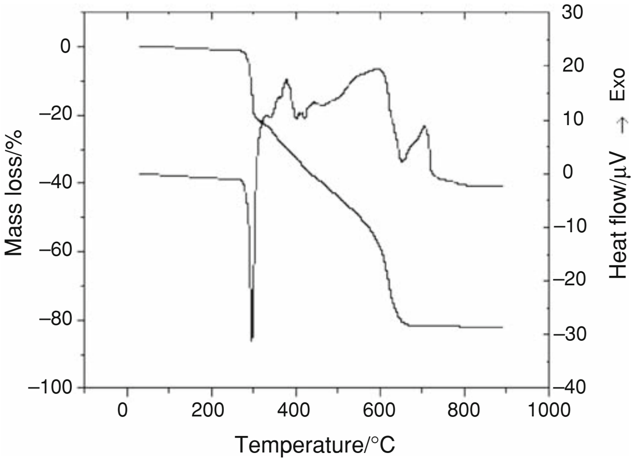

Fig. 3 TG and DTA curves of [Ni(L^1)] (**2**)

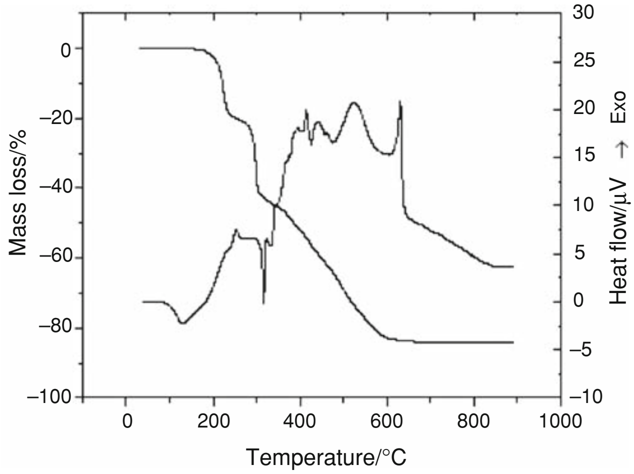

Fig. 4 TG and DTA curves of [Ni(L^2)] (**3**)

The anhydrous species (**5**) is very stable up to 210 °C (Fig. 6). After melting at 210 °C, the decomposition starts immediately and leads to CuO(CN)$_8$. The IR spectrum of this intermediate display the characteristic paracyanide bands together with a band at 472 cm^{-1} assigned to ν(Cu–O). The next step is an overlap of three processes and the mass variation corresponds to the paracyanide loss. The mass variation is in accord with the calculated one (found/calcd. overall mass loss: 79.8/80.2%).

For complex (**6**) the water is lost in the first step (Fig. 7) and the low temperatures corresponding to this step indicates its nature as crystallization one [23–26].

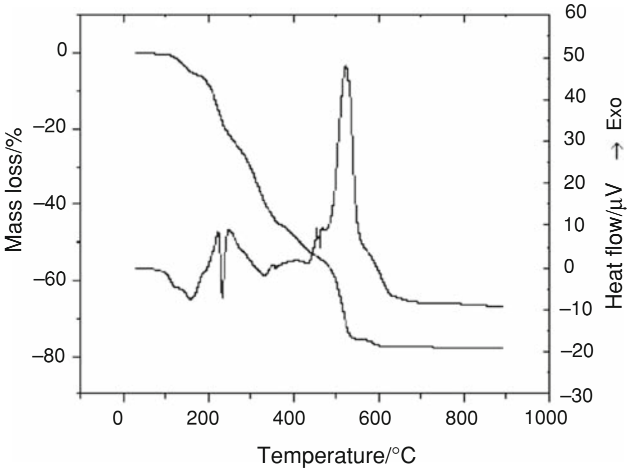

Fig. 5 TG and DTA curves of $[Cu(DMBG)_2]\cdot H_2O$ (**4**)

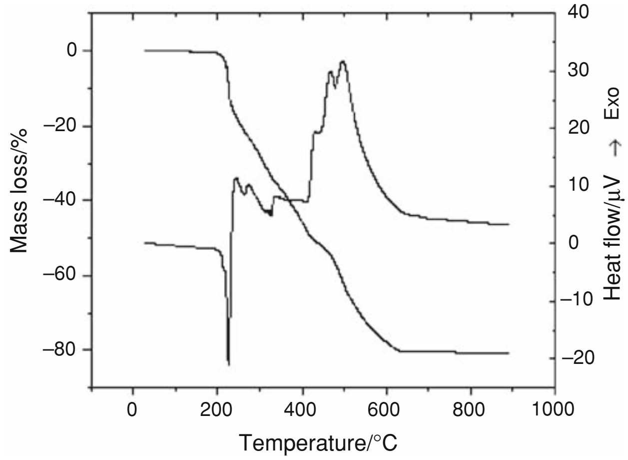

Fig. 6 TG and DTA curves of $[Cu(L^1)]$ (**5**)

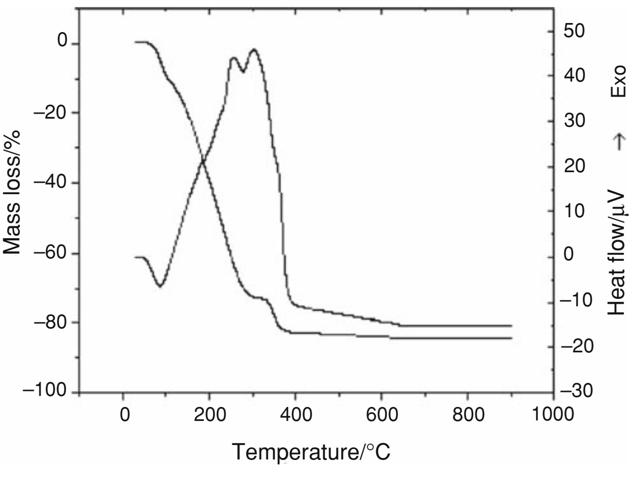

Fig. 7 TG and DTA curves of $[Cu(L^2)]\cdot 3H_2O$ (**6**)

In the IR spectrum of anhydrous complex isolated at 120 °C the band at 3420 cm^{-1} assigned to ν(OH) disappears. In the 120–300 °C range, the endothermic process with a mass loss of 61.84% is assigned to a large amount of ligand oxidation with $CuO(CN)_2$ formation (as the IR spectrum indicates). The last step is assigned also to paracyanide elimination in at least two processes with CuO stabilisation as final residue (found/calcd. overall mass loss: 83.0/83.6%).

Conclusions

Nickel(II) and copper(II) complexes with ligands bearing biguanide moiety were obtained by one pot condensation and characterised in order to develop new effective antimicrobial agents.

The IR spectra indicate the biguanide moieties coordination while the electronic spectra are consistent with a square-planar stereochemistry for all complexes.

Some compounds or intermediates melt before or during the thermal transformation that occur in two or three steps and comprise water elimination, biguanide moiety transformation as well as paracyanide decomposition. The final residue was metal(II) oxide in all cases as both IR and powder X-ray diffraction indicate.

References

1. Bailey CJ, Turner RC. Metformin. New Engl J Med. 2003;334:574–9.
2. Woo LCY, Yuen VG, Thompson KH, McNeill JH, Orvig C. Vanadyl-biquanide complexes as potential synergistic insulin mimics. J Inorg Biochem. 1999;76:251–7.
3. Bentefrit F, Morgant G, Viossat B, Leonce S, Guilbaud N, Pierre A, et al. Synthesis and antitumor activity of the mwtformin platinum(IV) complex. Crystal structure of the tetrachloro(metformin)platinum (IV) dimetrylsulfoxide solvate. J Inorg Biochem. 1997;68:53–9.
4. Olar R, Badea M, Cristurean E, Lazar V, Cernat R, Balotescu C. Thermal behavior spectroscopic and biological characterization of cobalt(II), zinc(II), palladium(II) and platinum(II) complexes with N,N-dimethylbiguanide. J Therm Anal Calorim. 2005;80:451–5.
5. Olar R, Badea M, Cristurean E, Parnau C, Marinescu D. Thermal behaviour of new N,N-dimethylbiguanide complexes having selective and effective antibacterial activity. J Therm Anal Calorim. 2006;84:53–8.
6. Olar R, Badea M, Lazar V, Balotescu C, Cristurean E, Marinescu D. Thermal behaviour of some N,N-dimethylbiguanide derivatives displaying antimicrobial activity. J Therm Anal Calorim. 2007;88:323–7.
7. Olar R, Badea M, Grecu MN, Marinescu D, Lazar V, Balotescu C. Thermal behavior, spectroscopic and biological characterization of copper(II) complexes with N, N-dimethylbiguanide. J Therm Anal Calorim. 2008;92:239–43.

8. Zhu M, Lu L, Yang P, Jin X. Bis(1,1-dimetrylbiguanido)nickel(II). Acta Crystallogr. 2002;E58:m272–4.
9. Zhu M, Lu L, Yang P, Jin X. Bis(1,1-dimetrylbiguanido)copper(II) octahydrate. Acta Crystallogr. 2002;E58:m217–9.
10. Bailey PJ, Pace S. The coordination chemistry of guanidines and guanidinates. Coord Chem Rev. 2001;214:91–141.
11. Loginova NV, Koval'chuk TV, Zheldakova RA, Osipovich NP, Sorokin VL, Polozov GI, et al. Synthesis and biological evaluation of copper (II) complexes of sterically hindered o-aminophenol derivatives as antimicrobial agents. Bioorganic Med Chem Lett. 2006;16:5403–7.
12. El-Ayaan U, El-Metwally NM, Youssef MM, El Bialy SAA. Perchlorate mixed–ligand copper(II) complexes of beta-diketone and ethylene diamine derivatives: thermal, spectroscopic and biochemical studies. Spectrochim Acta A. 2007;68:1278–86.
13. Khanmohammadi H, Arabahmadi R, Abnosi MH, Khavasi HR. Synthesis, crystal structure, spectral and biological studies of CuII–MII(M = Zn and Pb) heterodinuclear complexes of new phenol-based macrocyclic ligands. Polyhedron. 2007;26:4963–70.
14. Sreedaran S, Bharathi KS, Kalilur Rahiman A, Jagadish L, Kaviyarasan V, Narayanan V. Novel unsymmetrical macrocyclic dicompartmental binuclear copper(II) complexes bearing 4- and 6-coordination sites: Electrochemical, magnetic, catalytic and antimicrobial studies. Polyhedron. 2008;27:2931–8.
15. Kurtoğlu M, Ispir E, Kurtoğlu N, Serin S. Novel vic-dioximes: synthesis, complexation with transition metal ions, spectral studies and biological activity. Dyes Pigments. 2008;77:75–80.
16. Gudasi KB, Patil MS, Vadavi RS. Synthesis, characterization of copper(II), cobalt(II), nickel(II), zinc(II) and cadmium(II) complexes of [7-hydroxy-4-methyl-8-coumarinyl]glycine and a comparitive study of their microbial activities. Eur J Med Chem. 2008;43:2436–41.
17. Efthimiadou EK, Katsarou ME, Karaliota A, Psomas G. Copper(II) complexes with sparfloxacin and nitrogen-donor heterocyclic ligands: structure–activity relationship. J Inorg Biochem. 2008;102:910–20.
18. Chandra S, Gautam A, Tyagi M. Synthesis, structural characterization, and antibacterial studies of a tetradentate macrocyclic ligand and its Co(II), Ni(II), and Cu(II) complexes. Russ J Coord Chem. 2009;35:25–9.
19. Luo W, Meng X-G, Xiao F-P, Cheng G-Z, Ji Z-P. Synthesis, characterization and bioactivity of a new Fe(III) 18-metallacrown-6 and a new trinuclear linear Ni(II) complexes. Polyhedron. 2008;27:1802–8.
20. Babykutty PV, Prabhakaran CP, Anantaraman R, Nair CGR. Electronic and infrared spectra of biguanide complexes of the 3d-transition metals. J Inorg Nucl Chem. 1974;36:3685–8.
21. Nakamoto K. Infrared and Raman Spectra of inorganic and coordination compounds. New York: Wiley; 1986. p. 228–9.
22. Lever ABP. Inorganic electronic spectroscopy. Amsterdam: Elsevier; 1986. p. 507–54.
23. Modi CK, Patel MN. Synthetic, spectroscopic and thermal aspects of some heterochelates. J Therm Anal Calorim. 2008;94: 247–55.
24. Abou El-Enein SA. Polymeric and sandwich Schiff's bases complexes derived from 4,4′-methylenedianiline. Characterization and thermal investigation. J Therm Anal Calorim. 2008;91: 929–36.
25. Gaber M, Rehab AF, Badr-Eldeen DFS. pectral and thermal studies of new Co(II) and Ni(II) hexaaza and octaaza macrocyclic complexes. J Therm Anal Calorim. 2008;91:957–62.
26. Vikram L, Sivasankar BN. Hydrazinium metal(II) and metal(III) ethylenediamine tetraacetate hydrates. Spectral, thermal and XRD studies. J Therm Anal Calorim. 2008;91:963–70.